

# ON IRREGULAR LDPC CODES WITH QUANTIZED MESSAGE PASSING DECODING

Michael Meidlinger and Gerald Matz

Institute of Telecommunications, TU Wien (Vienna, Austria)

Email: {mmeidlin,gmatz}@nt.tuwien.ac.at

**Abstract**—Irregular low-density parity-check (LDPC) codes are among the best codes currently known. Unfortunately, the performance of existing codes may deteriorate substantially with practical finite-precision decoder implementations. This motivates us to extend our previous work on finite-alphabet decoders based on look-up tables (LUTs) to irregular LDPC codes. We devise a joint design of the LUTs used for different node degrees and present a strategy to optimize the degree distribution (DD) of the LDPC code under LUT decoding. Numerical simulations show that with 4-bit LUT decoding the resulting codes outperform state-of-the-art codes with floating point min-sum (MS) decoding.

## I. INTRODUCTION

*Background.* LDPC codes have excellent performance and are used in a wide variety of communication systems, notably wireless systems such as DVB-S2, WiMAX, and IEEE 802.11n. LDPC decoders use message passing (MP) schemes like the belief propagation (BP) and the MS algorithms, which involve real-valued (infinite precision) messages. Practical hardware implementations, however, require finite-precision message representations. Usually, the decoder messages are uniformly quantized with at least 5 bits since a lower precision deteriorates the error rate severely.

Recently, there has been significant interest in *finite alphabet* or *LUT* decoding of LDPC codes [1]–[5]. Rather than performing the conventional BP/MS arithmetics on quantized message representations, these decoders use suitably designed discrete mappings from incoming to outgoing messages, thereby neglecting the log-likelihood ratio (LLR) interpretation of messages. These approaches allow further reduction of the message bit-width while maintaining (and sometimes even outperforming) the error rate performance of traditional MP schemes.

In our previous work [6], we devised a hybrid min-LUT decoder and demonstrated its practical feasibility in [7], [8]. The min-LUT decoder can be viewed as combination of the MS algorithm and the LUT design of [9] and drastically reduces implementation complexity as compared to a purely LUT-based design.

*Contributions.* While existing work is limited to regular LDPC codes, we here investigate LUT decoding of *irregular* LDPC codes. Specifically, we advocate a LUT design that explicitly takes into account the code's DD. We derive an asymptotic stability condition in the spirit of [10] that leads to the conclusion that existing optimized DDs are ill-suited for LUT decoding. We thus propose an optimization of the DD for LUT decoding, which leads to irregular LDPC codes with

excellent performance and low decoding complexity. With a message resolution as low as 4 bits, LUT-based decoding of these codes is superior to conventional MS decoding at floating point precision.

## II. LDPC CODES AND DECODERS

We consider ensembles of binary LDPC codes represented by a Tanner graph consisting of  $N$  variable nodes (VNs) and  $M$  check nodes (CNs). The edges between VNs and CNs are characterized by the degree distributions [11]

$$\lambda(z) = \sum_{i \in \mathcal{D}_v} \lambda_i z^{i-1}, \quad \rho(z) = \sum_{j \in \mathcal{D}_c} \rho_j z^{j-1}. \quad (1)$$

Here  $\lambda_i$ ,  $i \in \mathcal{D}_v$ , is the probability that an edge is incident to a VN of degree  $i$ , and  $\rho_j$ ,  $j \in \mathcal{D}_c$ , is the probability that an edge is incident to a CN of degree  $j$ . In a regular  $(d_v, d_c)$  LDPC code, all VNs have degree  $d_v$  and all CNs have degree  $d_c$ .

LDPC codes are decoded using MP algorithms, where messages are exchanged between VNs and CNs over the course of several decoding iterations. At iteration  $\ell$ , the message from VN  $n$  (with degree  $i$ ) to an adjacent CN  $m$  are computed via a mapping  $\Phi_i^{(\ell)} : \mathcal{L} \times \overline{\mathcal{M}}_\ell^{i-1} \rightarrow \mathcal{M}_\ell$  according to

$$\mu_{n \rightarrow m} = \Phi_i^{(\ell)}(L_n, \bar{\mu}_{n \setminus m}). \quad (2)$$

Here,  $L_n \in \mathcal{L}$  denotes the channel LLR at VN  $n$  and  $\bar{\mu}_{n \setminus m} \in \overline{\mathcal{M}}_\ell^{i-1}$  is the vector of incoming messages from all adjacent CNs except  $m$  ( $\overline{\mathcal{M}}_\ell, \mathcal{M}_\ell$ , and  $\mathcal{L}$  are the message and LLR alphabets). Similarly, the message in iteration  $\ell$  from CN  $m$  (with degree  $j$ ) to an adjacent VN  $n$  is obtained via the mapping  $\bar{\Phi}_j^{(\ell)} : \mathcal{M}_\ell^{j-1} \rightarrow \overline{\mathcal{M}}_{\ell+1}$  defined by

$$\bar{\mu}_{m \rightarrow n} = \bar{\Phi}_j^{(\ell)}(\mu_{m \setminus n}), \quad (3)$$

where  $\mu_{m \setminus n} \in \mathcal{M}_\ell^{j-1}$  is the vector of messages incoming from the adjacent VNs except for VN  $n$ .

For the BP algorithm, all message alphabets equal the set of reals and the update mappings stay the same during iterations and are given by the algebraic expressions

$$\Phi_i^{\text{BP}}(L, \bar{\mu}) = L + \sum_{m=1}^{i-1} \bar{\mu}_m, \quad (4)$$

$$\bar{\Phi}_j^{\text{BP}}(\mu) = 2 \tanh^{-1} \left( \prod_{n=1}^{j-1} \tanh \left( \frac{\mu_n}{2} \right) \right), \quad (5)$$

whereas for the MS algorithm, (5) is replaced by

$$\bar{\Phi}_j^{\text{MS}}(\mu) = \prod_{n=1}^{j-1} \text{sign}(\mu_n) \cdot \min_n |\mu_n|. \quad (6)$$

Funding by WWTF Grant ICT12-054.

### III. SYMMETRIC LUT DECODING

In this section, we briefly discuss LUT decoding; further details can be found in [6], [12]. LUT decoding is based on finite message alphabets  $\mathcal{L}$ ,  $\mathcal{M}_\ell$  and  $\overline{\mathcal{M}}_\ell$  and uses LUTs instead of algebraic operations to implement the message updates. Since the CN update (6) preserves the message alphabet and can be efficiently implemented in hardware, we focus on LUT design for the VN update. Our LUT design is based on density evolution (DE) and maximization of the local information flow in the code's Tanner graph.

Consider a binary input discrete memoryless channel (DMC) that maps coded bits  $x \in \{-1, 1\}$  to discrete channel outputs  $L \in \mathcal{L} = \{L_1, \dots, L_{|\mathcal{L}|}\}$  according to transition probabilities  $p_{L|x}(L|x)$ . The elements  $L_m$  of  $\mathcal{L}$  are irrelevant from an information theoretic perspective and can be uniquely identified with their label  $m$ . The values  $L_m$  are assumed to satisfy the *LLR symmetry* condition (cf. [10, Def. 1])

$$L_m = \log \frac{p_{L|x}(L_m|+1)}{p_{L|x}(L_m|-1)}, \quad m = 1, \dots, |\mathcal{L}|. \quad (7)$$

For LUT decoding, we postulate that the elements  $\mu \in \mathcal{M}_\ell$  and  $\bar{\mu} \in \overline{\mathcal{M}}_\ell$  of the message alphabets satisfy a similar property, i.e.

$$\mu = \log \frac{p_{\mu|x}^{(\ell)}(\mu|+1)}{p_{\mu|x}^{(\ell)}(\mu|-1)}, \quad \bar{\mu} = \log \frac{p_{\bar{\mu}|x}^{(\ell)}(\bar{\mu}|+1)}{p_{\bar{\mu}|x}^{(\ell)}(\bar{\mu}|-1)}, \quad (8)$$

where  $p_{\mu|x}^{(\ell)}(\mu|x)$  and  $p_{\bar{\mu}|x}^{(\ell)}(\bar{\mu}|x)$  are the conditional probability mass functions (pmfs) of the messages (modeled as iid).

This modeling assumption on the one hand allows us to apply the symmetry concepts from [13] and on the other hand induces a sign-magnitude interpretation of the discrete messages such that the update rule (6) can still be applied, leading to a min-LUT decoder [6] which does not require a LUT for the CN message updates. To design the LUT for the VN updates (2), we follow the approach of [1], [9]. For notational simplicity, we suppress node degree and iteration index in what follows. The aim is to maximize the mutual information [14] between the message  $\Phi(L, \bar{\mu})$  (viewed as quantization from  $\mathcal{L} \times \overline{\mathcal{M}}^{i-1}$  to  $\mathcal{M}$ ) and the associated code bit  $x$ ,

$$\Phi^* = \arg \max_{\Phi \in \mathcal{Q}} I(\Phi(L, \bar{\mu}); x). \quad (9)$$

If the discrete inputs  $(L, \bar{\mu})$  to  $\Phi$  are sorted according to increasing LLRs, the separating hyperplane condition derived in [9] guarantees that the optimal  $\Phi$  has contiguous quantization regions. In order to solve (9), we need the joint distribution of channel LLR and incoming CN messages, which are determined using discrete DE as follows.

**Lemma 1** (Product pmfs [1]). *For a VN with  $i-1$  incoming, conditionally iid messages with distribution  $p_{\bar{\mu}|x}(\bar{\mu}|x)$  and conditionally iid channel LLR with distribution  $p_{L|x}(L|x)$ , the conditional joint message and LLR distribution is given by*

$$p_{L, \bar{\mu}|x}(L, \bar{\mu}|x) = p_{L|x}(L|x) \prod_{m=1}^{i-1} p_{\bar{\mu}_m|x}(\bar{\mu}_m|x). \quad (10)$$

For a CN with  $j-1$  incoming, conditionally iid messages with distribution  $p_{\mu|x}(\mu|x)$ , the conditional joint message distribution is given by

$$p_{\mu|x}(\mu|x) = 2^{2-j} \sum_{\mathbf{x} \in \mathcal{P}_x} \prod_{n=1}^{j-1} p_{\mu_n|x}(\mu_n|x_n), \quad (11)$$

with  $\mathcal{P}_x \triangleq \{\mathbf{x} \in \{-1, 1\}^{j-1} : \prod_{n=1}^{j-1} x_n = x\}$ .

The required LLRs can be calculated using the LLRs of the individual input messages via the following result, whose proof can be found in [12].

**Theorem 1.** *For given CN-to-VN messages  $\bar{\mu} = (\bar{\mu}_1, \dots, \bar{\mu}_{i-1})$  and channel LLR  $L$ , the LLR of the combination is given by*

$$\log \frac{p_{L, \bar{\mu}|x}(L, \bar{\mu}|+1)}{p_{L, \bar{\mu}|x}(L, \bar{\mu}|-1)} = L + \sum_{m=1}^{i-1} \bar{\mu}_m. \quad (12)$$

For given VN-to-CN messages  $\mu = (\mu_1, \dots, \mu_{j-1})$ , the LLR of the combination is given by

$$\log \frac{p_{\mu|x}(\mu|+1)}{p_{\mu|x}(\mu|-1)} = 2 \operatorname{atanh} \left( \prod_{n=1}^{j-1} \tanh \left( \frac{\mu_n}{2} \right) \right). \quad (13)$$

In summary, given a channel  $p_{L|x}(L|x)$ , discrete DE iteratively computes the product pmfs and LLRs according to Lemma 1 and Theorem 1, and solves the optimization problem (9), yielding the message pmf for the next iteration as well as the LUT mapping  $\Phi_i^{(\ell)}$ .

### IV. LUT DESIGN FOR IRREGULAR CODES

For regular LDPC codes, all nodes have identical degrees and thus only one update (quantization) rule  $\Phi$  is required in each iteration. This is no longer true for irregular LDPC codes, where distinct mappings (LUTs)  $\Phi_i : \mathcal{L} \times \overline{\mathcal{M}}^{i-1} \rightarrow \mathcal{M}$  need to be designed for each node degree  $i$ . A straightforward approach would be to optimize these mappings separately, i.e.,

$$\max_{\Phi_i} I(\Phi_i(L, \bar{\mu}); x). \quad (14)$$

This approach, however, does not take into account the code's DD (cf. (1)), i.e., the fact that certain degrees occur much more frequently than others. Thus, we propose to design the LUTs according to

$$\arg \max_{\Phi} I(\Phi(L, \bar{\mu}, d); x), \quad (15)$$

where  $\Phi(L, \bar{\mu}, d)$  assigns an output message to any input combination  $(L, \bar{\mu})$  and random degree  $d$  with DD  $\lambda(z)$  (see (1)). Hence, the resulting  $\Phi$  can then be decomposed into individual mappings  $\Phi_i$  for all node degrees  $i$  and the distribution used to compute the mutual information in (15) is given by

$$p_{L, \bar{\mu}, d|x}(L, \bar{\mu}, d|x) = \lambda_i p_{L, \bar{\mu}|d,x}(L, \bar{\mu}|d, x). \quad (16)$$

The optimization itself is then performed along the same lines as described in the previous section, yielding a jointly optimal set of mappings  $\Phi = \{\Phi_1, \dots, \Phi_i\}$  for a given DD.

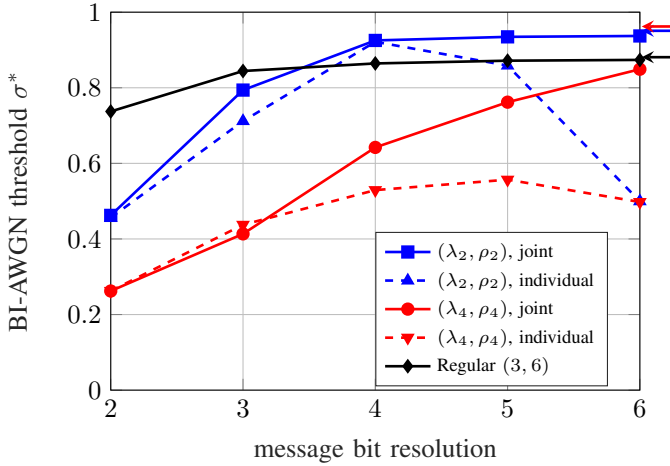


Fig. 1: DE thresholds versus message resolution for different LDPC ensembles in a BI-AWGN channel with individual and joint LUT design. Arrows on the right margin indicate the corresponding BP thresholds.

The performance difference between the individual design (14) and the joint design (15) can be significant. Fig. 1 shows the DE thresholds [11, Sec. 4.7] for irregular LDPC codes with DD from Table I obtained with the two LUT design strategies in a binary input additive white Gaussian noise (BI-AWGN) channel. It is seen that the DE thresholds for the individual LUT design (14) are worse than those of the joint design (15) and even decrease for larger message alphabets (higher quantizer resolutions), thereby confirming the superiority of the joint LUT design.

## V. DEGREE DISTRIBUTIONS FOR LUT DECODING

Another insight offered by Fig. 1 is as follows. For the  $(\lambda_4, \rho_4)$  ensemble (taken from [10]), the DE threshold with jointly designed LUTs falls substantially short of the BP threshold even at high resolutions. This indicates that these codes are ill-suited for LUT decoding. Similar observations have been made in [15]. The authors of that paper also showed how irregular DDs can be designed to take into account and mitigate the effects of quantization in MS decoding.

In what follows, we set out to find DDs that are optimized for LUT decoding. To this end, special attention is paid to the degree 2 VNs. Due to the minimal extrinsic information they receive, they are the most difficult to decode, especially for quantized extrinsic information. For the case of BP decoding, the decisive role of degree 2 edges has been quantified in [10] by means of an asymptotic stability analysis, providing upper bounds on the fraction of degree 2 edges (the probability of degree 2 edges in the  $(\lambda_4, \rho_4)$  ensemble from [10] is indeed fairly close to that bound). Since LUT decoding can be viewed as a degraded form of BP, it seems intuitive that the fraction of degree 2 edges should be lower for LUT decoding. To quantify this line of reasoning, we consider the all-ones codeword and a linearization of the CN-to-VN message pmfs around the fixed point  $\Delta_\infty$ . Starting from a VN-to-CN message pmf

$$q_0 \triangleq 2\epsilon\Delta_0 + (1 - 2\epsilon)\Delta_\infty, \quad (17)$$

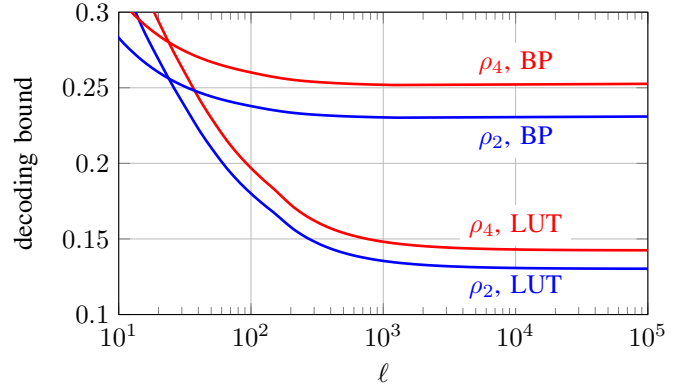


Fig. 2: Decoding bound convergence for BP and 4-bit LUT decoding and two CN degree distributions from Table I in a BI-AWGN channel with  $\sigma = 0.929$ .

we can show that for too large fraction of degree 2 edges, the error probability associated with any message pmf of the type (17) is necessarily bounded away from 0, i.e., there exists  $\xi > 0$  such that  $P_e(q_0) \geq \xi$ .

**Lemma 2.** Consider a degree distribution  $(\lambda, \rho)$ , a symmetric channel pmf  $p_0$ , and a message pmf of the form (17). Furthermore, define

$$r \triangleq - \lim_{\ell \rightarrow \infty} \frac{1}{\ell} \log P_e(p_0^{(\ell)}), \quad (18)$$

where  $p_0^{(\ell)} = Q_\ell(p_0^{(\ell-1)}) \otimes p_0$  for some sequence of quantizers  $\{Q_\ell\}_{\ell=1}^\infty$ . Then if  $\lambda'(0)\rho'(1) > e^r$ , there exists  $\xi > 0$  such that  $P_e(q_0) \geq \xi$ .

The proof of this result is given in [12], and for the quantizer sequence, we use mutual information (MI)-optimized update rules (9). It uses the analogy between LUT and BP decoding established in Theorem 1 and follows the lines of [10, Theorem 5].

Note that for BP decoding, Lemma 2 holds for arbitrary message pmfs, providing a sharp boundary between stable and unstable DDs. Unfortunately, such a general statement appears impossible for LUT decoding. However, as we will see in what follows, the upper bound  $\lambda'(0) = \lambda_2 \leq \lambda_2^* \triangleq e^r/\rho'(1)$  can still be used for searching LUT-optimized DDs. Furthermore, for BP decoding the decoding bound can be explicitly expressed as [10]

$$r = \int_{\mathbb{R}} p_0(x) e^{-x/2} dx. \quad (19)$$

Unfortunately, we couldn't find a similar expression for the decoding bound under LUT decoding. Fig. 2 shows the convergence behavior of the decoding bound for both decoder types. As expected, LUT decoding tolerates fewer degree-2 nodes. Furthermore, the limit can be determined numerically with about  $10^4$  iterations.

We next investigate the problem of finding a degree distribution  $(\lambda, \rho)$  with maximum DE threshold under LUT decoding for a given target rate  $R$ . We follow the hill climbing approach of [16], taking into account the decoding bound  $\lambda_2^*$  derived previously.

$l$	$\lambda_l(x)$	$\rho_l(x)$	$\sigma_{\text{LUT}}^*$	$\sigma_{\text{BP}}^*$
1	$0.16385x + 0.40637x^2 + 0.42978x^7$	$0.59105x^6 + 0.40876x^7 + 0.00019x^8$	0.89657	0.91775
2	$0.13805x + 0.40104x^2 + 0.02659x^8 + 0.43433x^{16}$	$0.32338x^7 + 0.67662x^8$	0.92919	0.95075
3	$0.30013x + 0.28395x^2 + 0.41592x^7$	$0.22919x^5 + 0.77081x^6$	0.583182	0.9497
4	$0.23802x + 0.20997x^2 + 0.03492x^3 + 0.12015x^4 + 0.01587x^6 + 0.00480x^{13} + 0.37627x^{14}$	$0.98013x^7 + 0.01987x^8$	0.603642	0.9622

**TABLE I:** Degree distributions pairs  $(\lambda, \rho)$  for rate  $\frac{1}{2}$  codes and DE thresholds for a BI-AWGN under LUT and BP decoding. The pairs 1 and 2 have been optimized for LUT decoding of quantized BI-AWGN channels using the method described in Algorithm 1, pairs 3 and 4 are taken from [10] and have been optimized for BP decoding. For the LUT DE thresholds, a resolution of 4 bits and the min-LUT algorithm has been used.

More specifically, we start with an initial degree distribution with rate  $R < R_t$  and iteratively solve linear programs (LPs) that maximize the code rate. Note that

$$R = 1 - \frac{\sum_j \frac{\rho_j}{j}}{\sum_i \frac{\lambda_i}{i}} \quad (20)$$

and thus  $R$  can be maximized by minimizing  $\sum_j \frac{\rho_j}{j}$  or maximizing  $\sum_i \frac{\lambda_i}{i}$ , both of which are linear in the DDs. Additional linear constraints are necessary to limit the search space to the space of pmfs, to limit the step size to ensure linearity, and to guarantee that updated DDs improve the error probability/threshold. Additionally, for the VN DD we also impose  $\lambda_2 \leq \lambda_2^*$ . The linear program to update the VN distribution can be stated as follows:

$$\text{maximize } \sum_{i \in \mathcal{D}_v} \frac{\lambda_i}{i} \quad (21)$$

subject to

$$\sum_{i \in \mathcal{D}_v} \lambda_i = 1, \quad (22)$$

$$\lambda_i \geq 0, \quad i \in \mathcal{D}_v, \quad (23)$$

$$\lambda_2 \leq \lambda_2^*, \quad (24)$$

$$\left| P_\ell - \sum_{i \in \mathcal{D}_v} P_{\ell|i} \lambda_i \right| \leq \delta (P_{\ell-1} - P_\ell)^+, \quad (25)$$

$$\sum_{i \in \mathcal{D}_v} P_{\ell|i} \lambda_i \leq P_{\ell-1}. \quad (26)$$

Here,  $P_{\ell|i}$  corresponds to the VN-to-CN message error probability for iteration  $\ell$  and node degree  $i$  (assuming DE with the current DD to be improved by solving the LPs). For the CN DD a similar LP can be formulated using CN-to-VN message error probabilities  $Q_{\ell|j}$ .

Algorithm 1 summarizes the procedure for DD optimization. Note that for the DE runs in lines 4 and 6, there is the possibility that DE does not converge with sufficient precision for the updated DDs. When this happens, we reduce the channel noise and rerun DE until convergence.

## VI. SIMULATION RESULTS

### A. Decoder Performance

Fig. 3 compares different decoders in terms of frame error rate (FER) after 100 decoding iterations versus signal to noise ratio (SNR) for an irregular rate  $1/2$  LDPC code of length

### Algorithm 1 DD optimization for LUT decoding

**Input:** initial DD  $(\lambda, \rho)$  with rate  $R$ , target rate  $R_t > R$ , step size  $\delta$ , LUT resolution  $N_q$

1: compute DE threshold  $\sigma(\lambda, \rho, N_q)$

2: **while**  $R < R_t$  **do**

3:   compute  $\lambda_2^*(\sigma, \rho, N_q)$

4:   run DE and save probabilities  $P_\ell, P_{\ell|i}$

5:   update  $\lambda$  by solving the VN LP

6:   run DE and save probabilities  $Q_\ell, Q_{\ell|j}$

7:   update  $\rho$  by solving the CN LP

8:   compute updated rate  $R(\lambda, \rho)$

9: **end while**

**Output:** optimized DD pair  $(\lambda, \rho)$  for rate  $R_t$

$N = 10000$  obtained from the DD  $(\lambda_2, \rho_2)$  in Table I using the progressive edge growth algorithm [17]. As expected, (unquantized) BP has the best performance. Consistent with DE threshold results, the min-LUT decoder performs slightly worse. With 4-bit messages, min-LUT decoding is within about 0.2 dB of BP decoding. In order to further reduce complexity, we implemented a min-LUT decoder in which LUTs are reused on average for 4 decoding iterations rather than designing a dedicated LUT for each iteration. While this reduces the complexity by  $\frac{4}{5} \hat{=} 80\%$ , the FER performance is only slightly worse than without reuse. A substantial performance loss (0.55 dB from BP) occurs only after the LUT message resolution is reduced to 3 bit. We also included BP results for a regular (3, 6) code decoded at floating point precision for comparison. Even with 4-bit LUT decoding, the irregular code outperforms the BP-decoded regular (3, 6) code. This is in agreement with the DE results in Fig. 1: the LUT threshold of  $(\lambda_2, \rho_2)$  is below the BP threshold of the (3, 6) code for 3 bits of resolution but outperforms the regular code for 4 or more bits.

### B. Performance of Irregular, LUT optimized Codes

Next, we assess the performance of LUT decoders with LUT optimized codes in a practical scenario. By using the LUT optimized DD  $(\lambda_1, \rho_1)$  in (20), we created a code with similar degree structure as the rate  $1/2$  DVB-S2 LDPC code. Note that the degree structure of the DVB-S2 code approximately matches the BP optimized DD  $(\lambda_3, \rho_3)$ , and thus, due to the low threshold, cannot be expected to perform well with LUT decoding. We compare the two codes for

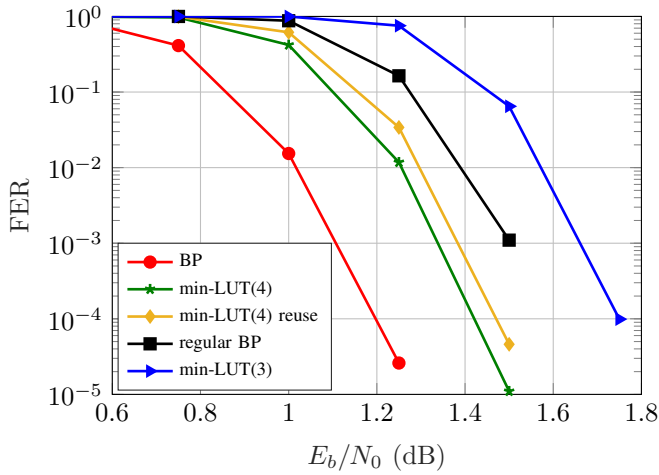


Fig. 3: FER Simulations for different codes of length  $N = 10000$  and 100 decoding iterations

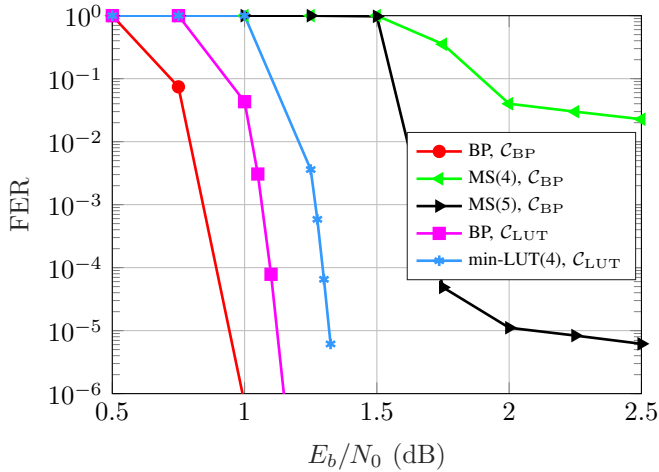


Fig. 4: FER Simulations for the LUT optimized code  $C_{LUT}$  and the BP optimized DVB-S2 code  $C_{BP}$ . For for both codes  $N = 64800$  and for all decoders 100 decoding iterations have been performed.

different decoding algorithms in Fig. 4. As we can see, the DVB-S2 code using BP performs best. However, quantized MS decoding with 4 and 5 bits entails a huge performance degradation and high error floors, which could be mitigated to some extent by using improved MS decoders [18]. For higher resolutions up to floating point precision (not shown), the water fall region remained unchanged (only the error floors vanished). In contrast, the LUT-optimized code with 4-bit min-LUT decoding performs much closer to the BP-decoded DVB-S2 code (BP decoding of the LUT-optimized code is only marginally better than LUT decoding). We conclude that a LUT-optimized code with 4-bit min-LUT decoding is capable of outperforming a MS decoder using a standard compliant code at floating point precision by roughly 0.5 dB.

## VII. CONCLUSION

We extended the concept of LUT decoding to irregular LDPC codes. A jointly optimal design for LUTs corresponding to different node degrees was proposed; this design explicitly accounts for the code's DD. We further found that codes with

DDs optimized for BP decoding have low thresholds under LUT decoding due to lack of asymptotic stability. We thus developed a stability bound for LUT decoding and proposed an algorithm for optimizing DDs for LUT decoding. This allowed us to devise LUT-optimized irregular LDPC codes. We presented error rate simulations indicating that LUT-optimized codes perform well under both BP and LUT decoding and showed that with 4-bit LUT decoding these optimized codes can outperform conventional codes with floating point MS decoding.

Further details of the proposed designs for LUT decoders (like reuse and implementation of LUTs) and for optimizing the code's DD are provided in [12].

## REFERENCES

- [1] B. Kurkoski, K. Yamaguchi, and K. Kobayashi, "Noise thresholds for discrete LDPC decoding mappings," in *Proc. IEEE GLOBECOM 2008*, New Orleans, LA, USA, Nov. 2008, pp. 1–5.
- [2] J. Lewandowsky and G. Bauch, "Trellis based node operations for LDPC decoders from the information bottleneck method," in *Proc. Int. Conf. Signal Process. Comm. Systems*, Cairns, Australia, Dec. 2015, pp. 1–10.
- [3] J. Lewandowsky, M. Stark, and G. Bauch, "Optimum message mapping LDPC decoders derived from the sum-product algorithm," in *Proc. IEEE ICC 2016*, Kuala Lumpur, Malaysia, May 2016, pp. 1–6.
- [4] S. Planjery, D. Declercq, L. Danjean, and B. Vasic, "Finite alphabet iterative decoders – Part I: Decoding beyond belief propagation on the binary symmetric channel," *IEEE Trans. Communications*, vol. 61, no. 10, pp. 4033–4045, Oct. 2013.
- [5] F. J. C. Romero and B. M. Kurkoski, "Decoding LDPC codes with mutual information-maximizing lookup tables," in *Proc. IEEE ISIT 2015*, Hong Kong, China, Jun. 2015, pp. 426–430.
- [6] M. Meidlinger, A. Balatsoukas-Stimming, A. Burg, and G. Matz, "Quantized message passing for LDPC codes," in *Proc. 49th Asilomar Conf. Signals, Systems and Computers*, Pacific Grove, CA, USA, Nov. 2015.
- [7] A. Balatsoukas-Stimming, M. Meidlinger, R. Ghanaatian, G. Matz, and A. Burg, "A fully-unrolled LDPC decoder based on quantized message passing," in *Proc. SiPS 2015*, Hang Zhou, China, Oct. 2015.
- [8] R. Ghanaatian, A. Balatsoukas-Stimming, C. Muller, M. Meidlinger, G. Matz, A. Teman, and A. Burg, "A 0.594 Tbps LDPC decoder based on finite-alphabet message passing," *submitted to IEEE Trans. VLSI*, 2017.
- [9] B. Kurkoski and H. Yagi, "Quantization of binary-input discrete memoryless channels," *IEEE Trans. Information Theory*, vol. 60, no. 8, pp. 4544–4552, Aug. 2014.
- [10] T. Richardson, M. Shokrollahi, and R. Urbanke, "Design of capacity-approaching irregular low-density parity-check codes," *IEEE Trans. Information Theory*, vol. 47, no. 2, pp. 619–637, Feb. 2001.
- [11] T. Richardson and R. Urbanke, *Modern coding theory*. Cambridge University Press, 2008.
- [12] M. Meidlinger and G. Matz, "Quantized symmetric message passing for LDPC codes," *submitted to IEEE Trans. Communications*, 2017.
- [13] T. Richardson and R. Urbanke, "The capacity of low-density parity-check codes under message-passing decoding," *IEEE Trans. Information Theory*, vol. 47, no. 2, pp. 599–618, Feb. 2001.
- [14] T. M. Cover and J. A. Thomas, *Elements of information theory*, 2nd ed. Wiley-Interscience, 2006.
- [15] B. Smith, F. R. Kschischang, and W. Yu, "Low-density parity-check codes for discretized min-sum decoding," in *Proc. 23rd Biennial Symposium on Communications*, Kingston, ON, Canada, May 2006, pp. 14–17.
- [16] S.-Y. Chung, J. Forney, G.D., T. Richardson, and R. Urbanke, "On the design of low-density parity-check codes within 0.0045 dB of the Shannon limit," *IEEE Communications Letters*, vol. 5, no. 2, pp. 58–60, Feb. 2001.
- [17] X.-Y. Hu, E. Eleftheriou, and D. Arnold, "Regular and irregular progressive edge-growth tanner graphs," *IEEE Trans. Information Theory*, vol. 51, no. 1, pp. 386–398, Jan. 2005.
- [18] J. Chen, A. Dholakia, E. Eleftheriou, M. Fossorier, and X.-Y. Hu, "Reduced-complexity decoding of LDPC codes," *IEEE Trans. Communications*, vol. 53, no. 8, pp. 1288–1299, Aug. 2005.